

LDA and GGA calculations for high-pressure phase transitions in ZnO and MgO

John E. Jaffe, James A. Snyder, Zijing Lin, and Anthony C. Hess

Materials Sciences Department, Pacific Northwest Laboratory, Richland, Washington 99352

(Received 6 December 1999; revised manuscript received 17 March 2000)

We report total energy and electronic structure calculations for ZnO in the B4 (wurtzite), B3 (zinc blende), B1 (rocksalt), and B2 (CsCl) crystal structures over a range of unit cell volumes. We employed both the local-density approximation (LDA) and the PBE96 form of the generalized gradient approximation (GGA) together with optimized Gaussian basis sets to expand the crystal orbitals and periodic electron density. In agreement with earlier *ab initio* calculations and with experiment, we find that the B4 phase of ZnO is slightly lower in energy than the B3 phase, and that it transforms first to the B1 structure under applied pressure. The equilibrium transition pressure p_{T1} is 6.6 GPa at the LDA level of theory and 9.3 GPa in the GGA, compared to experimental values around 9 GPa. This confirms a trend seen by other workers in which the LDA underestimates structural transition pressures which are more accurately predicted by the GGA. At much higher compression, we predict that the B1 phase of ZnO will transform to the B2 (cesium chloride) structure at $p_{T2} = 260$ GPa (LDA) or 256 GPa (GGA) indicating that gradient corrections are small for this material at megabar pressures. This is the first quantitative prediction of this transition in ZnO, and should be testable with diamond-anvil techniques. We predict that ZnO remains a semiconductor up to p_{T2} . For comparison we find that the B1 to B2 transition in MgO occurs at 515 GPa with either LDA or GGA, in excellent agreement with other *ab initio* predictions.

I. INTRODUCTION

ZnO is a wide band gap semiconductor with a range of technological applications including electronic and electro-optic devices, catalysts, chemical sensors, and conductive solar cell window layers. There is also continuing interest in the high-pressure behavior of ZnO for geophysical as well as fundamental materials physics reasons. It has been known experimentally¹ since 1962 that under increasing hydrostatic pressure, the B4 (hexagonal wurtzite) low-pressure phase of ZnO transforms to the cubic B1 (rocksalt or NaCl) structure at a pressure in the vicinity of $p_{T1} = 9$ GPa. Recent experimental work has probed the B1 phase of ZnO by synchrotron x-ray diffraction^{2,3} and by combined x-ray diffraction and Mössbauer spectroscopy.⁴ The maximum pressure attained in any experiment on ZnO to date is 56 GPa,² and the B1 phase remained stable up to this pressure. On the theoretical side there have been several first-principles studies of the B1 phase and B4-B1 phase equilibrium in ZnO using the linear combination of Gaussian-type orbitals (LCGTO) Hartree-Fock (HF) method,⁵ the full-potential linear muffin-tin orbital approach⁶ to density-functional theory (DFT) within the local-density and generalized gradient approximations (LDA and GGA), linear augmented plane wave⁴ (LAPW) LDA, HF,⁷ and correlated HF³ perturbed ion models, and LCGTO-LDA and GGA methods.³ These calculations were mostly limited to the same pressure range as the experiments, and did not consider any possible structures of ZnO except B1, B3, and B4. However, it has been suggested⁸ that at sufficiently high pressure, ZnO should undergo a phase transformation from the sixfold-coordinated B1 (cubic NaCl) to the eightfold-coordinated B2 (cubic CsCl) structure, in analogy to the alkali halides and alkaline-earth oxides. Hence, the main goal of the present paper is to predict the equilibrium transition pressure p_{T2} between the B1 and B2 phases of ZnO, the equation-of-state of the B2 phase, and the elec-

tronic structure of the material above and below the transition.

A second major goal is to assess the relative accuracy of the LDA and the GGA for DFT calculations on high-pressure properties of ZnO, considered as an example of a partially ionic semiconductor. Other workers⁹ have found that the LDA significantly underestimates phase-transition pressures for several metallic and (predominantly) covalent systems, and that the GGA yields better agreement with experiment. A study of ZnO from the standpoint of gradient corrections to DFT will provide more data on this issue. We also have calculated the equations-of-state of the B1 and B2 phases of MgO and the transition pressure between them, as an example of an even more ionic solid and as a test of the accuracy of our method.

II. METHOD OF CALCULATION

The calculations described here were performed with a three dimensionally periodic implementation of the Kohn-Sham density-functional theory. Two different levels of approximation in the exchange-correlation (XC) functional were used: the LDA as parametrized by Vosco, Wilk, and Nusair¹⁰ (VWN) and the GGA of Perdew, Burke, and Ernzerhof¹¹ (PBE96). The single-electron Kohn-Sham eigenfunctions (crystal Bloch orbitals) are expanded in a set of contracted atom-centered Gaussian-type orbitals (GTO) adapted from standard molecular DFT basis sets¹² by reoptimization of the most diffuse GTO's in the crystalline environment. For purposes of treating the Coulomb interactions, the charge density is also expanded in uncontracted Gaussians,¹² and long-ranged Coulomb interactions are treated by a form of the Ewald convention. This LCAO-type method permits basis sets and integral techniques to be carried over from quantum chemistry with only modest changes, and helps in achieving accurate all-electron calculations that scale well with system size. Our method has been

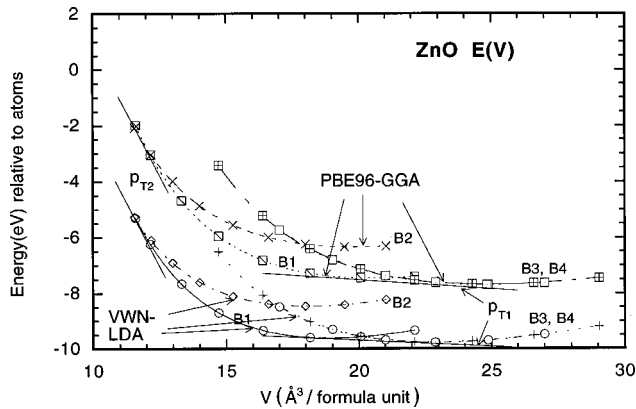


FIG. 1. Energy versus volume per formula unit for ZnO in the B4, B3, B1, and B2 structures, showing the common tangent construction for transition pressures.

described in detail elsewhere,¹³ and Boettger and Trickey¹⁴ have described an LCGTO method very similar to ours, except for the technique for the numerical integration over the exchange-correlation (XC) potential and energy density. In our¹⁵ XC integrations, the multicenter integrals are decomposed into sums of one-center numerical integrals on radial and angular grids centered on the atomic nuclei, and the integration points and weights are adapted to the functional behavior of the charge density near the nuclei.

A standard self-consistent field procedure with density matrix mixing was employed in this paper, and the resulting total energies as functions of volume were fitted to the Murnaghan¹⁶ equation-of-state (EOS) to obtain the bulk modulus and other structural parameters. Cohesive energies were found by subtracting the total energy per ZnO formula unit of the solid at its equilibrium lattice constant from the energy of the corresponding isolated atoms. The same functionals and code were used for the atoms as for the solids by increasing the lattice constants to several hundred Ångstrom, with appropriate spin states and unmodified molecular-orbital and density basis functions for the atomic calculations. For the B4 (wurtzite) phase of ZnO, the c/a ratio and internal parameter u were fully relaxed to their minimum-energy values at each unit cell volume considered, using total energies and *ab initio* forces^{13,17} from our code. Relativistic corrections, finite (room) temperature, and zero-point motion were not included and are not expected to have large effects on our main results.

III. RESULTS FOR ZnO

Total energy versus volume data for the B4, B3, B1, and B2 phases of ZnO are shown in Fig. 1 for both the VWN-LDA and PBE96-GGA functionals. Volume and energy are per single ZnO formula unit in all cases (there are two formula units per unit cell for wurtzite, and one per primitive unit cell for the other structures). The zero of energy is taken as the sum of the energies of isolated neutral O and Zn atoms as described above, so that the absolute value of the energy at the minimum of each curve gives our prediction for the equilibrium cohesive energy of the corresponding phase of ZnO. Common-tangent lines have been added to indicate equilibria between B4 and B1, and also B1 and B2 phases with each functional; note that the curves for the B3 (zinc

blende) and B4 phases are indistinguishable on the scale of the figure. The negative of the slope of each common tangent gives the equilibrium pressure for the associated transition (hysteresis and metastability are not addressed by this analysis). The curves through each set of $E(V)$ points are obtained by fitting the Murnaghan¹⁶ EOS to each set of data. The fit to the data is almost perfect in every case, indicating that a somewhat different choice of volume points or a different model equation-of-state would have given essentially the same results for the EOS parameters given in Table I. This table also contains results of previous first-principles calculations³⁻⁵ as well as experimental^{1,2,4,18,19} data. The overall agreement with experiment and earlier theory is very good, with the LDA showing the usual cohesive overbinding and slightly too small lattice constants, while the GGA corrects the cohesive energy but overcorrects the lattice constants, and also predicts the somewhat too small bulk moduli. The latter discrepancy may be due in part to the neglect of relativistic effects.²⁰

Because it is difficult to extract accurate slopes from the common-tangent lines shown in Fig. 1, we have inverted the Murnaghan expression for $p(V) = -dE/dV$ to obtain $V(p)$ and used it to find the enthalpy $H(p) = E + pV$ for each phase. The transition pressures are then obtained from the enthalpy curve crossings, i.e., $H_{B4}(p_{T1}) = H_{B1}(p_{T1})$ and $H_{B1}(p_{T2}) = H_{B2}(p_{T2})$. Our results for transition pressures, volumes, and volume changes are given in Table II along with experimental^{2,4} and previous theoretical^{4,5} data for the B4 to B1 transition, which is the only one observed or quantitatively predicted to date for ZnO. We find that the LDA predicts the B4 to B1 transition at 6.6 GPa, while the GGA result for this pressure is 9.3 GPa. The latter is in good agreement with the experimental values (for increasing pressure; due to hysteresis, the transition back to the B4 phase occurs at much lower pressure as the pressure is decreasing) and also with the earlier Hartree-Fock prediction. Our results thus show a trend noted⁹ for other materials, in which structural transition pressures are underestimated by the LDA but accurately predicted by the GGA. All calculations and experiments agree that there is a volume reduction across the B4 to B1 transition of about 17%. At a much higher pressure, we predict a transition from B1 to B2 ZnO near 2.6 Mbar (260 GPa) accompanied by a volume reduction of about 5%. The LDA and GGA transition pressures agree to about 1.5% (probably less than the numerical uncertainty of these pressures) indicating that gradient corrections to the LDA are relatively small in this material at megabar pressures. Though high, such pressures can be attained in modern diamond-anvil cells.

IV. COMPARISON WITH MgO

To assess the quantitative reliability and qualitative material dependence of our predictions about ZnO, we now turn to a calculation of the B1 to B2 transition pressure in MgO. We employ the same basis set for oxygen as before, and a magnesium basis set of similar design and quality to that used for Zn, along with identical computational conditions and techniques. Our predictions for MgO Murnaghan¹⁶ EOS parameters and B1 to B2 transition quantities are given in Table III along with predictions²¹⁻²⁴ by other authors and experimental^{23,25-28} properties of the B1 (rocksalt) phase of

TABLE I. Murnaghan equation-of-state parameters for B4 (wurtzite), B3 (zinc blende), B1 (rocksalt), and B2 (CsCl) phases of ZnO. All extensive quantities are per ZnO formula unit. Conventional cubic lattice constants a are related to equilibrium volumes by $V_0 = a^3/4$ (B1, B3) and $a^3/2$ (B2). For the B4 structure $V_0 = \sqrt{3}a^2c/4$ and c/a and the internal displacement u are also given.

	LDA	GGA	Other LDA ^a	Hartree-Fock	Experiment
B4					
E_{coh} (eV)	9.769	7.692		5.658 ^b	7.52 ^c
V_0 (\AA^3)	22.874	24.834		24.570 ^b	23.810, ^d 23.790 ^a
B_0 (GPa)	162.3	133.7	160	154.4 ^b	142.6, ^d 183 ^a
B'	4.05	3.83	4.4	3.6 ^b	3.6, ^d 4 ^a
c/a	1.6138	1.6076	1.604	1.593 ^b	1.6021, ^d 1.6018 ^a
u	0.3790	0.3802	0.381	0.3856 ^b	0.3823, ^e 0.3819 ^f
B3					
E_{coh} (eV)	9.754	7.679		5.606 ^b	
V_0 (\AA^3)	22.914	24.854		24.551 ^b	
B_0 (GPa)	161.7	135.3		156.8 ^b	
B'	3.95	3.72		3.6 ^b	
B1					
E_{coh} (eV)	9.611	7.455		5.416 ^b	
V_0 (\AA^3)	18.904	20.502		19.799, ^b 18.8547 ^g	19.60, ^d 19.484 ^a
B_0 (GPa)	205.7	172.7	205	203.3, ^b 132 ^g	202.5, ^d 228 ^a
B'	3.90	3.68	4.88	3.6, ^b 3.8 ^g	3.54, ^d 4 ^a
B2					
E_{coh} (eV)	8.462	6.334			
V_0 (\AA^3)	18.073	19.785			
B_0 (GPa)	194.3	156.9			
B'	3.99	3.77			

^aReference 4 (LAPW-LDA and experiment).

^bReference 5 (LCGTO-HF).

^cReference 18.

^dReference 2.

^eReference 1.

^fReference 19.

^gReference 3 (HF-PI model).

MgO. For equilibrium properties we find reasonable agreement between our calculations and earlier ones and with experiment for the B1 phase of MgO. Our prediction for the B1 to B2 transition pressure in MgO is 515 GPa with either the LDA or the GGA, again showing the smallness of gradient corrections at high pressure in ionic materials. This transition pressure agrees very well with the LAPW-LDA result of Mehl²² *et al.* and the recent pseudopotential LDA work of Karki *et al.*²¹ The earlier LDA paper by Chang and Cohen²³ predicted a much higher transition pressure while the

Hartree-Fock transition pressure of Causa *et al.*²⁴ is much lower. We presume that these early studies^{23,24} were less accurate. The good agreement with other recent work for MgO suggests that our predictions for ZnO are probably also accurate.

V. ELECTRONIC STRUCTURE OF HIGH-PRESSURE ZnO

We have calculated the total density-of-states DOS and band structure at the LDA level of theory for ZnO at five

TABLE II. Data for phase transition B4→B1 (T_1) and B1→B2 (T_2) in ZnO.

	LDA	GGA	Other LDA	Hartree-Fock	Experiment
p_{T_1} (GPa)	6.60	9.32	14.5 ^a	8.57 ^b	9.1, ^c 8.7 ^a
$V_{B_1}(p_{T_1})$ (\AA^3)	22.029	23.346		23.358 ^b	22.481, ^c 22.783 ^a
$V_{B_1}(p_{T_1})$ (\AA^3)	18.341	19.515		19.037 ^b	18.799, ^c 18.804 ^a
ΔV_1 (\AA^3)	3.688	3.831		4.321 ^b	3.682, ^c 3.979 ^a
p_{T_2} (GPa)	260	256			
$V_{B_1}(p_{T_2})$ (\AA^3)	11.977	12.340			
$V_{B_2}(p_{T_2})$ (\AA^3)	11.377	11.738			
ΔV_2 (\AA^3)	0.600	0.602			

^aReference 4 (LAPW-LDA and experiment).

^bReference 5 (LCGTO-HF).

^cReference 2.

TABLE III. Murnahan EOS parameters and phase transition data for MgO.

	LDA	GGA	Other LDA	Hartree-Fock ^d	Experiment
B1					
$E_{\text{coh}}(\text{eV})$	11.817	10.045	9.96 ^c	7.27	10.33, ^c 10.45 ^e
$V_0(\text{\AA}^3)$	18.034	19.156	19.199, ^a 18.088, ^b 18.403 ^c	18.535	18.671 ^f
$B_0(\text{GPa})$	185.9	169.1	159.7, ^a 172, ^b 146 ^c	186	156, ^g 162 ^b
B'	3.40	3.28	4.26, ^a 4.09 ^b	3.53	4.7, ^g 4.08 ^b
B2					
$E_{\text{coh}}(\text{eV})$	10.296	8.537	8.454 ^c	5.50	
$V_0(\text{\AA}^3)$	17.573	18.740	18.150 ^c	17.034	
$B_0(\text{GPa})$	169.8	152.6		193	
B'	3.54	3.39		2.94	
$p_T(\text{GPa})$	515	515	451, ^a 515, ^b 1050 ^c	220	
$V_{B1}(p_T)(\text{\AA}^3)$	9.053	9.223	9.877, ^a 8.96, ^b 6.938 ^c	11.65	
$V_{B1}(p_T)(\text{\AA}^3)$	8.764	8.907	9.429, ^a 8.54, ^b 6.607 ^c	10.39	
$\Delta V(\text{\AA}^3)$	0.289	0.316	0.448, ^a 0.42, ^b 0.331 ^c	1.26	

^aReference 21 (PPW-LDA).^bReference 22 (LAPW-LDA).^cReference 23 (PPW-LDA).^dReference 24 (LCGTO-HF).^eReference 25.^fReference 26.^gReference 27.^hReference 28.

different structures or densities: (i) the B4 phase at zero pressure; (ii) the B4 phase just below the first transition at p_{T1} ; (iii) the B1 phase just above p_{T1} ; (iv) the B1 phase just below p_{T2} ; and (v) the B2 phase just above p_{T2} . We show the ZnO total DOS for cases (i)–(iii) in Fig. 2(a) and for cases (iv) and (v) in Fig. 2(b). Figure 2(a) shows that when wurtzite ZnO is compressed, the peak at the top of the upper valence band is slightly reduced in height and shifted down in energy, the O 2s- and Zn 3d-derived peaks are slightly broadened and shifted up in energy, and a splitting appears in the Zn 3d states. Also, the overall upper valence bandwidth is slightly reduced. The changes in the B4 phase band structure over the range $p=0$ to p_{T1} are thus seen to be fairly small. However, on transforming to the B1 structure at p_{T1} , more significant changes occur, in particular, the peak near the valence-band maximum is greatly reduced in height. The Zn 3d peak also becomes narrower, and the O 2s-derived states drop slightly in energy.

Upon compression of the B1 phase ZnO through the wide pressure range from p_{T1} to p_{T2} , the upper valence band broadens greatly, the splitting of the Zn 3d peak in the DOS shows a large increase, and the O 2s-derived band moves down in energy and broadens. The fundamental band gap also increases with increasing pressure in this range. With the B1→B2 transition, the upper valence bandwidth remains almost unchanged but the peak near the valence-band maximum reappears. The structure of the Zn 3d states changes radically (in fact they appear to be heavily hybridized with the O 2p-derived states) and the O 2s-derived states broaden further and shift up in energy.

The band structures provide insight into the origin of the

DOS features just mentioned. Cases (i), (iii), and (v) are shown in Figs. 3–5, respectively. [Cases (ii) and (iv) are qualitatively similar to (i) and (iii), respectively, and are not shown.] There are two key concepts that govern the response of the ZnO band structure to compression and changed atomic coordination: (a) changes in nearest-neighbor bondlengths as they affect overlaps and bandwidths and (b) changes in symmetry as they affect p - d hybridization and band repulsion. As the neighboring atoms approach each other on compression of the solid, basis functions (and orbitals in a Hückel-like picture) overlap more strongly, producing increased dispersion of the electron bands in k space and consequently increased bandwidths along the energy axis. However, when there is a phase transition to a structure of increased coordination, the nearest-neighbor bonds lengthen even though the density is increased. The behavior of the bandwidths up to p_{T2} reflects these considerations. However, the band structures reveal further qualitative changes that occur with the change of symmetry at the structural transitions. Where the symmetry permits hybridization of O 2p and Zn 3d-derived bands, there is effectively a repulsion between them, which pushes the anion 2p states upwards, an effect previously noted in both binary²⁹ and ternary³⁰ semiconductors. In the tetrahedrally coordinated B4 phase (Fig. 3) this repulsion is present throughout the Brillouin zone, but in the cubic B1 (Fig. 4) and B2 (Fig. 5) structures it is suppressed near the gamma point³¹ as a result of the inversion symmetry through the atomic center. As a result, the highest valence bands are repelled upwards near the zone boundaries but not at the zone center, so that the valence-band maximum now occurs at the zone boundary rather than at the gamma

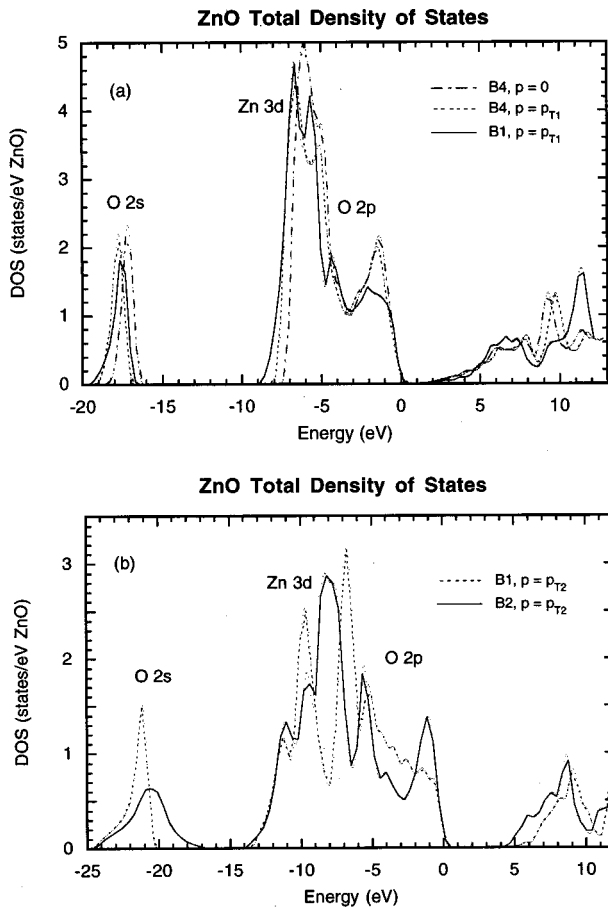


FIG. 2. Total DOS for ZnO in (a) the B4 structure at $p=0$ and p_{T1} and the B1 structure at $p=p_{T1}$, and (b) the B1 and B2 structures at $p=p_{T2}$.

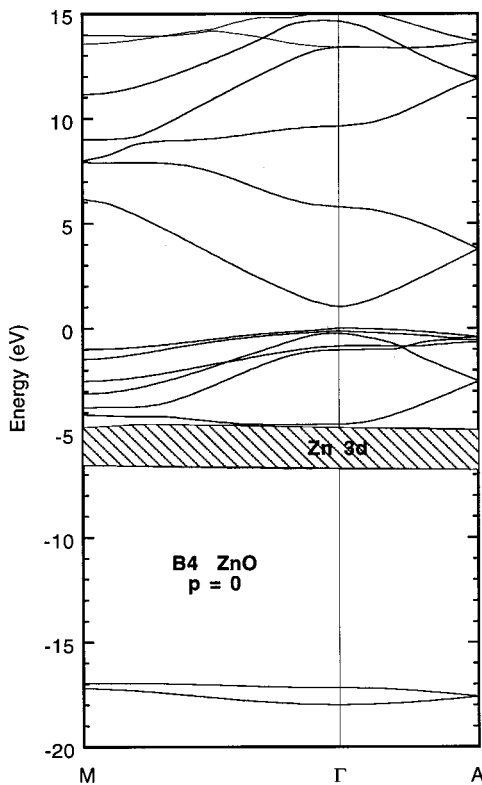


FIG. 3. Band structure for ZnO in the B4 structure at $p=0$.

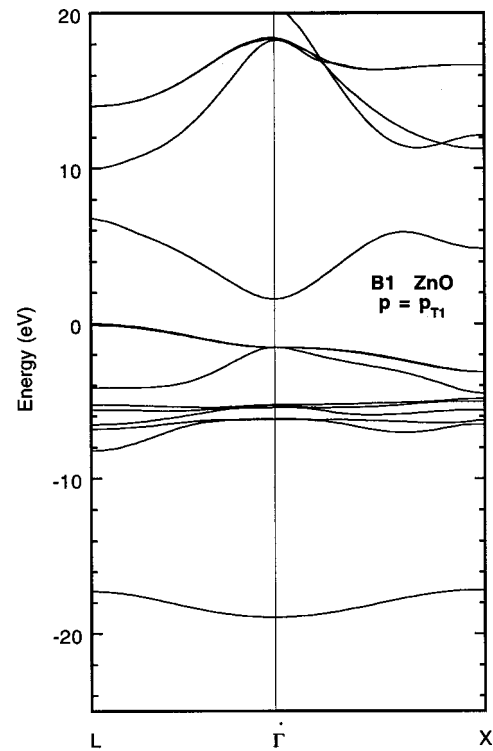


FIG. 4. Band structure for ZnO in the B1 structure at $p=p_{T1}$.

point. This accounts for the change in shape of the band edge seen in the total DOS plots. There is also a change in the form of the Zn 3d-derived bands, which are now narrowest near the gamma point as a result of the suppressed hybridization there. In the B2 structure the Zn 3d and O 2p states are completely hybridized and cannot be disentangled.

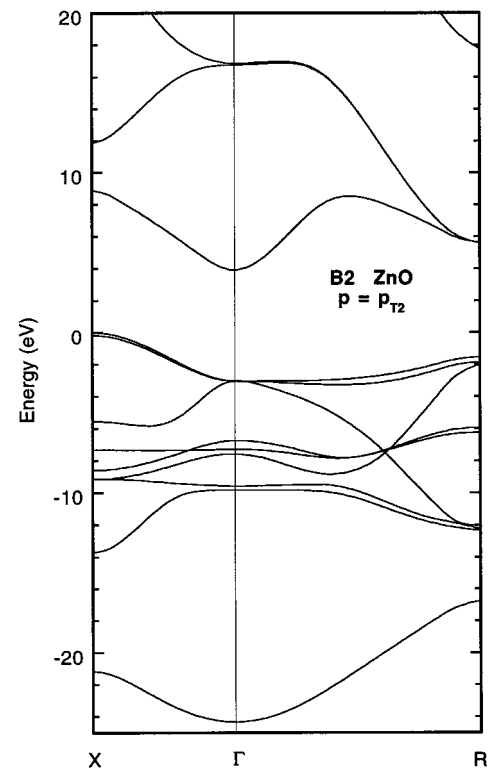


FIG. 5. Band structure for ZnO in the B2 structure at $p=p_{T2}$.

VI. DISCUSSION AND CONCLUSION

Our key result is that ZnO will transform from the rock-salt (B1) structure to the CsCl (B2) structure at a pressure near 2.6 Mbar, assuming no other new phase appears first. It should be possible to attain this transition in a diamond-anvil cell, and to examine the electronic properties of this material through the transition. We also confirm that the GGA corrects the tendency of the LDA to underestimate transition pressures between low-pressure phases, but find that gradient corrections are unimportant at high pressures. When we study the high-pressure behavior of MgO by the same approach as we have used for ZnO, we find results consistent with other recent first-principles studies. Note that we have used the “standard methodology”³² of guessing a few candidate high-pressure structures and comparing their enthalpies. We have no guarantee against metastability with respect to other possibly lower-energy structures or even dynamic instability, through soft phonons or other mechanisms, leading to new phases. However, there are strong empirical grounds for expecting the B4(B3)→B1→B2 transition sequence with increasing pressure in ionic, wide-gap materials

like most II–VI compounds. Other structures, such as NiAs or diatomic β -Sn in place of NaCl or InBi or AuCd in place of CsCl, are more likely in the *metallic* high-pressure phases of less ionic, narrower-gap semiconductors including most III–V and column IV materials. We have predicted that a large band gap persists to the highest pressures considered in ZnO (and MgO) despite that the LDA (and GGA) band gaps are expected always to be smaller than experiment. Hence there is a reasonable chance that the B1→B2 transition can actually be observed in ZnO. Of course high-pressure phonon calculations would be an interesting future extension of the present paper and could still uncover unstable modes in ZnO at some pressure.

ACKNOWLEDGMENTS

We acknowledge discussions with Dominic Alfonso and Maciej Gatoski, and the support of the Office of Energy Research, Division of Geosciences of the U.S. Department of Energy. Pacific Northwest National Laboratory is operated for the U.S. Department of Energy by Battelle Memorial Institute under Contract No. DE-AC06-76RLO1830.

-
- ¹C. H. Bates, W. B. White, and R. Roy, *Science* **137**, 993 (1962); W. Class, A. Ianucci, and H. Nesor, *Norelco Rep.* **13**, 87 (1966).
- ²S. Desgreniers, *Phys. Rev. B* **58**, 14 102 (1998).
- ³J. M. Recio, M. A. Blanco, V. Luaña, R. Pandey, L. Gerward, and J. S. Olsen, *Phys. Rev. B* **58**, 8949 (1998).
- ⁴H. Karzel, W. Potzel, M. Köfferlein, W. Schiessl, M. Steiner, U. Hiller, G. M. Kalvius, D. W. Mitchell, T. P. Das, P. Blaha, K. Schwartz, and M. P. Pasternak, *Phys. Rev. B* **53**, 11 425 (1996).
- ⁵J. E. Jaffe and A. C. Hess, *Phys. Rev. B* **48**, 7903 (1993).
- ⁶R. Ahuja, L. Fast, O. Eriksson, J. M. Wills, and B. Johansson, *J. Appl. Phys.* **83**, 8065 (1998).
- ⁷J. M. Recio, R. Pandey, and V. Luaña, *Phys. Rev. B* **47**, 3401 (1993).
- ⁸L.-gun Liu and W. A. Bassett, *Elements, Oxides, and Silicates. High-Pressure Phases with Implications for the Earth's Interior* (Oxford University, New York, 1986).
- ⁹A. Zupan, P. Blaha, K. Schwarz, and J. P. Perdew, *Phys. Rev. B* **58**, 11 266 (1998); D. R. Hamann, *Phys. Rev. Lett.* **76**, 660 (1996).
- ¹⁰S. H. Vosko, L. Will, and M. Nusair, *Can. J. Phys.* **58**, 1200 (1980).
- ¹¹J. P. Perdew, K. Burke, and M. Ernzerhof, *Phys. Rev. Lett.* **77**, 3865 (1996); J. P. Perdew, K. Burke, and Y. Wang, *Phys. Rev. B* **54**, 16 533 (1996).
- ¹²N. Godbout, D. R. Salahub, J. Andzelm, and E. Wimmer, *Can. J. Chem.* **70**, 560 (1992), and unpublished. The auxiliary density basis was modified from its molecular form only by the removal of unnecessary, extremely small-exponent Gaussians. Detailed information on the basis sets used in the present calculation will be furnished on request.
- ¹³J. E. Jaffe and A. C. Hess, *J. Chem. Phys.* **105**, 10 983 (1996).
- ¹⁴J. C. Boettger and S. B. Trickey, *Phys. Rev. B* **51**, 15 623 (1995); **53**, 3007 (1996).
- ¹⁵Z. Lin, J. E. Jaffe, and A. C. Hess, *J. Phys. Chem. A* **103**, 2117 (1999).
- ¹⁶F. D. Murnaghan, *Proc. Natl. Acad. Sci. USA* **30**, 244 (1944).
- ¹⁷P. Pulay, *Mol. Phys.* **17**, 197 (1969).
- ¹⁸Deduced from experimental Zn heat of vaporization, ZnO enthalpy of formation and O₂ binding energy in *CRC Handbook of Chemistry and Physics*, 58th ed. (CRC, Boca Raton, 1977).
- ¹⁹J. Albertsson, S. C. Abrahams, and Å. Kvik, *Acta Crystallogr.* **45**, 34 (1989).
- ²⁰V. L. Moruzzi and P. M. Marcus, *Phys. Rev. B* **48**, 7665 (1993); J. Boettger, *J. Phys.: Condens. Matter* **11**, 3237 (1999).
- ²¹B. B. Karki, L. Stixrude, S. J. Clark, M. C. Warren, G. J. Ackland, and J. Crain, *Am. Mineral.* **82**, 51 (1997).
- ²²M. J. Mehl, R. E. Cohen, and H. Krakauer, *J. Geophys. Res.* **93**, 8009 (1988); **94**, 1977 (1989). We cite their static-lattice results from the Hedin-Lunqvist XC functional, which is numerically very close to the VWN LDA functional employed in our paper. Mehl *et al.* also give zero-point and finite temperature corrections, which are on the order of 1% for MgO, as expected.
- ²³K. J. Chang and M. L. Cohen, *Phys. Rev. B* **30**, 4774 (1984).
- ²⁴M. Causà, R. Dovesi, C. Pisani, and C. Roetti, *Phys. Rev. B* **33**, 1308 (1986).
- ²⁵E. S. Gaffney and T. J. Ahrens, *J. Chem. Phys.* **51**, 1088 (1969).
- ²⁶R. W. G. Wyckoff, *Crystal Structure* (Wiley, New York, 1963), p. 88.
- ²⁷H. K. Mao and P. M. Bell, *J. Geophys. Res.* **84**, 4533 (1979).
- ²⁸A. Chopelas, *Phys. Chem. Miner.* **23**, 25 (1996).
- ²⁹A. Zunger and S.-H. Wei, *Phys. Rev. B* **37**, 8958 (1988).
- ³⁰J. E. Jaffe and Alex Zunger, *Phys. Rev. B* **27**, 5176 (1983); **29**, 1882 (1984).
- ³¹K. Maschke and U. Rössler, *Phys. Status Solidi* **28**, 577 (1968); J. E. Jaffe, R. Pandey, and A. B. Kunz, *Phys. Rev. B* **43**, 14 030 (1991).
- ³²V. Ozolins and A. Zunger, *Phys. Rev. Lett.* **82**, 767 (1999); K. Kim, V. Ozolins, and A. Zunger, *Phys. Rev. B* **60**, R8449 (1999).